Steady State Response of Systems Modelled by Multibond Graphs

Gilberto Gonzalez-A[1], Noe, Barrera[2], Gerardo Ayala[3], Erasmo Cadenas[4]
Faculry of Electrical Engineering[1], Graduate Studies Division of the Faculty of Mechanical Engineering[1,4]
University of Michoacan[1,4]
Technological Institute of Morelia[2]
School of Sciences of Engineering and Technology, Autonomous University of Baja California[3]
gilmichga@yahoo.com.mx[1], noebg20@gmail.com[2], mr.gerardo.a@ieee.org[3]

Abstract: Multibond graph models has been introduced for the modelling of multibody systems for Breedveld and Tiernego [2, 5]. However, these publised papers do not give general methodologies to obtain the mathematical models. Hence, a junction structure of multibond graph models is proposed. In addition, the steady state response of systems modelled by multibond graphs in a derivative causality assignment is obtained. An example applying the propose methodology is solved.

Key–Words: Bond graph, Multibond graph, Multibody systems.

1 Introduction

By its nature a power conserving description of a system, the bond graph method is especially practical when several physical domains have to be modelled within a system simultaneously, or when the physics of domains other that one´s won specialty have to be understood. This is certainly the case in robotics where mechanic, hydraulic, pneumatic and electric systems in several combinations are present [2].

Clearly, modelling of the 3D motion of multibody systems is essential in robotics as well as for the analysis of vehicle dynamics in the automobile industry. There are numerous bond graph related publications in each of the two fields. The following papers are cited: in [2] a method to model mechanical systems with multibond graphs is described In [3] it presents a technique which produces explicit Lagrange or Hamilton equations for mechanism dynamics suitable for computer solution.

A bond graph model is derived for the geometric constraints of a three-axis flight table in [4]. In [5] it proposes the multibond graph notation in a concise way to represent the behavior of energy, power, entropy and other physical properties of macroscopic multiport systems. In [6] describes the history of the bond graph description of rigid body rotation dynamics and resolves a paradox that resulted from the common Euler Junction Structure (EJS) description of the exterior product in the Newton-Euler equation describing rigid body rotation. In [7] decomposition rules are derived for multiport-transformers, -resistors, -storage elements and -gyrators into 1- and 2-port elements, junctions and bonds.

The steady state response is an important characteristic of a system, for example, some equipment in electrical machines or in power electrical systems requires to know the steady state values for calibration. A procedure to determine the equilibrium state of a bond graph model is proposed in [10]. The equilibrium state of a system applying the bicausality to a bond graph model is presented in [11]. The steady state of a system with singular state matrix in the physical domain is proposed in [12].

In this paper, a junction structure of a multibond graph model is proposed. The state equation by using this junction structure for multibody systems modelled by multibond graphs is presented.

New results to determine structural properties for multibody systems based on the proposed junction of multibond graphs can be found.

Section 2 describes the typical modelling in bond graph. The modelling of systems with multibond graphs is developed in Section 3. The main result of this paper (scheme of multibond graphs using blocks and junction structure) is presented in this section. The proposed methodology is applied to two examples in Section 4. Finally, Section 5 gives the conclusions.

2 Modelling in Bond Graph

When two components are connected, power interactions are always present. Because power could flow in either direction, a sign convention for describing the power variables is necessary . In the bond language, the power variables are called effort $e\left(t\right)$ and flow $f\left(t\right)$. The power $P\left(t\right)$ flowing into or out of a port can be expressed as the product of an effort and a flow variable. Fig 1 shows the graphical representation of a bond [8].

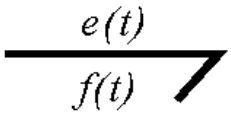

Fig. 1: Power bond.

The power variables for some physical systems are indicated on table 1.

Table 1. Power variables.

System	Effort (e)	Flow (f)
Mechanical	Force (F) Torque (τ)	Velocity (ν) Ang. velocity (ω)
Electrical	Voltage (v)	Current (i)
Hydraulic	Pressure (P)	Volume flow rate (Q)

Also, bond graph has energy variables called momentum $p\,(t)$ and displacement $q\,(t)$. The momentum is defined as the time integral of an effort and the displacement is the time integral of a flow variable.

At each port, both an effort and a flow exist, if one of the effort or flow variable is an input, the other will be the output, the relationship is called causality. Hence, effort and flow are in opposite directions. The causal stroke is represented by a short and perpendicular line made at one end of a bond and the causal stroke indicate the direction in which the effort signal is directed which is shown in Fig. 2 [8].

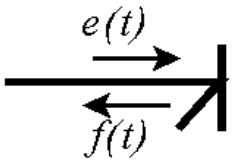

Fig. 2: Causal bond.

Also, the sources, dissipation and storage elements can be modelled in bond graph and table 2 gives these elements with causal relations.

Table 2. Causal forms for 1-ports.

Element	Causal Form	Causal Relation
Effort source	MSe ⟶	$e(t)=E(t)$
Flow source	MSf ⟶	$f(t)=F(t)$
Resistance	R ⟵	$e=\Phi_R(f)$
	R ⟵	$f=\Phi_R^{-1}(e)$
Capacitance	C ⟵	$e=\Phi_c^{-1}(\int f dt)$
	C ⟵	$f=d\Phi_c(e)/dt$
Inertance	I ⟵	$f=\Phi_I^{-1}(\int e dt)$
	I ⟵	$e=d\Phi_I(f)/dt$

3 State Space for a System based on Multibond Graphs

A multiport element may store energy and consequently be power discontinuous, or it may be power continuous. Analogous to the storage of electrical energy and charge in an ideal electrical capacitor, the energetic multiport element will be called multiport capacitor. Also, analogous to an isothermal electrical resistor, the isothermal entropic, non-energetic, power discontinuous (dissipation of free energy) multiport element will be called multiport resistor. Power and flow discontinuous multiport element is called multiport source, which is a collection of 1-port sources. According to the current bond graph terminology, all non-energetic, power continuous, non-entropic multiport elements belong to a multiport element called generalized junction structure [2, 5].

Efforts $\underline{e}\,(t)$ and flows $\underline{f}\,(t)$ in a multibond graph are usually written above or below, to the left or to right of the corresponding multibond respectively, Although this representation has been called a vector bond notation it is not a vector but merely a composition of the three bonds, corresponding to the three perpendicular axes, in one multibond. The equivalent bond graph representations as shown in Fig. 3 [2, 5].

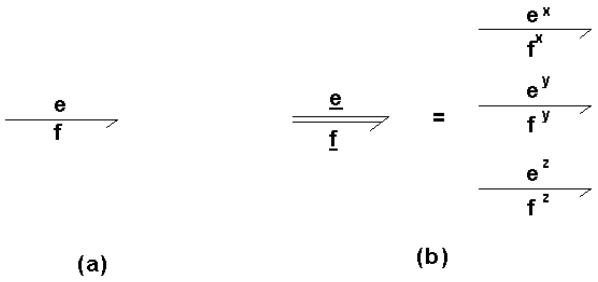

Fig. 3: Bonds; (a) Single bond; (b) Multibond.

The powerflow is now defined as $P = \underline{e}^T \underline{f}$, where $\underline{e}^T$ is the transpose of the column vector

$$\underline{e} = \begin{bmatrix} e^x \\ e^y \\ e^z \end{bmatrix} \text{ and } \underline{f} = \begin{bmatrix} f^x \\ f^y \\ f^z \end{bmatrix}$$

A simple multibond graph indicating the variables is shown in Fig. 4 [5].

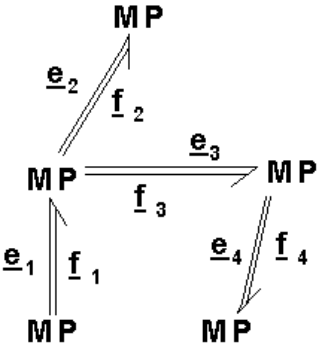

Fig. 4: Multibond graph with efforts and flows.

Multibond graph notation for single port elements $(MS_e, MS_f, I,\ C, R)$ is shown in Fig. 5.

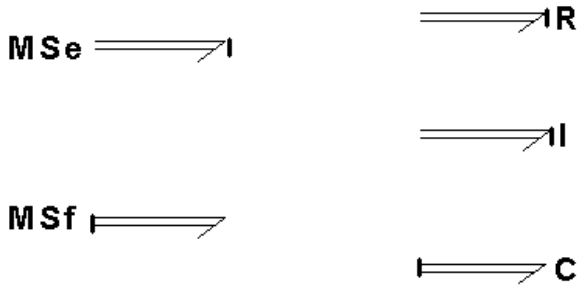

Fig. 5: Multibond graph elements.

A special emphasis to consider multiport gyrators is done in this paper whose constitutive relation for a multiport gyrator shown in Fig. 6 is [5]

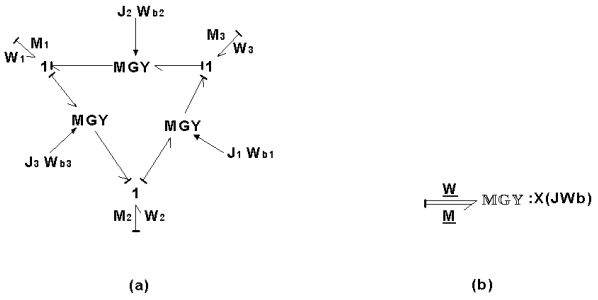

Fig. 6: Eulerian junction structure.

$$\underline{M} = \begin{bmatrix} M_1 \\ M_2 \\ M_3 \end{bmatrix} = X\left(Jw_b\right)\underline{w} = \begin{bmatrix} 0 & J_3w_{b3} & -J_2w_{b2} \\ -J_3w_{b3} & 0 & J_1w_{b1} \\ J_2w_{b2} & -J_1w_{b1} & 0 \end{bmatrix}\begin{bmatrix} w_1 \\ w_2 \\ w_3 \end{bmatrix}$$

where $w_b = \begin{bmatrix} w_{b1} & w_{b2} & w_{b3} \end{bmatrix}^T$ is constant.

A multibond graph can be organized into interconnected blocks (modulated sources, storage block, dissipation block, junction structure). Hence, a scheme of a multiport system represented by a multibond graph in a predefined integral causality assignment and key vectors is shown in Fig. 7

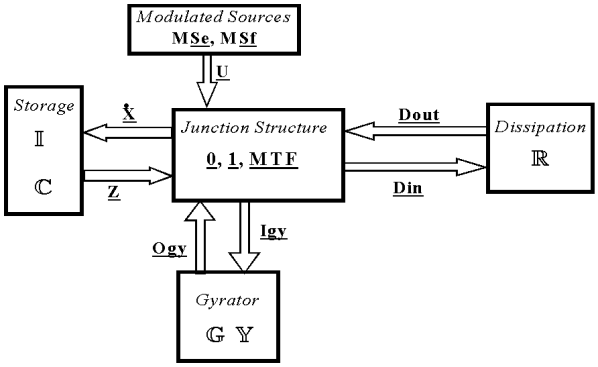

Fig. 7: Junction structure and key vectors of a multibond graph.

In Fig. 7, $\left(\underline{MS_e}, \underline{MS_f}\right)$ represents the effort and flow modulated multiport sources, storage block for linear multiport elements is $(\mathbb{C}, II)$, dissipation block for linear multiport resistors is $\mathbb{R}$ and $(\underline{0}\ , \underline{1}, \underline{MTF})$ are the $\underline{0}$ and $\underline{1}$ junctions and $\underline{MTF}$ denotes the multiport transformers; the multiport gyrators are defined by GY. The energy variables $\underline{p}$ and $\underline{q}$ are associated with II and $\mathbb{C}$ multiport elements in integral causality assignment that represent the states variables $\underline{x} \in \Re^{\underline{n}}$, $\underline{z} \in \Re^{\underline{n}}$ is the co-energy vector; $\underline{u} \in \Re^{\underline{p}}$ denotes the plant inputs; $\underline{I_{GY}} \in \Re^{\underline{s}}$ and $\underline{O_{GY}} \in \Re^{\underline{s}}$ are the inputs and outputs of the multiport gyrators, and $\underline{D_{in}} \in \Re^{\underline{r}}$ and $\underline{D_{out}} \in \Re^{\underline{r}}$ denote the relation between the dissipation multiport and the junction structure.

The mathematical model of a multibody system based on a multibond graph is determined by the junction structure

$$\begin{bmatrix} \dot{\underline{x}} \\ \underline{I_{GY}} \\ \underline{D_{in}} \end{bmatrix} = \begin{bmatrix} \mathbf{S}_{11}^{11} & \mathbf{S}_{11}^{12} & \mathbf{S}_{12}^{11} & \mathbf{S}_{13}^{11} \\ \mathbf{S}_{11}^{21} & \mathbf{S}_{11}^{22} & \mathbf{S}_{12}^{21} & \mathbf{S}_{13}^{21} \\ \mathbf{S}_{21}^{11} & \mathbf{S}_{21}^{12} & \mathbf{S}_{22} & \mathbf{S}_{23} \end{bmatrix} \begin{bmatrix} \underline{z} \\ \underline{O_{GY}} \\ \underline{D_{out}} \\ \underline{u} \end{bmatrix} \tag{1}$$

the entries of $\mathbf{S}$ take values inside the set $\{0, \pm\mathbf{I},\ \pm\mathbf{K}_t\}$ where $\mathbf{K}_t$ is the transformer module and the constitutive relations for the multiport elements are

$$\underline{z} = \mathbf{F}\underline{x} \tag{2}$$

$$\underline{O_{GY}} = \mathbf{X}_{GY}\underline{I_{GY}} \tag{3}$$

$$\underline{D_{out}} = \mathbf{L}\underline{D_{in}} \tag{4}$$

From the second and third lines of (1) with (3) and (4)

$$\underline{I_{GY}} = \left(\mathbf{I} - \mathbf{S}_{11}^{22}\mathbf{X}_{GY}\right)^{-1}\left(\mathbf{S}_{11}^{21}\underline{z} + \mathbf{S}_{12}^{21}\mathbf{L}\underline{D_{in}} + \mathbf{S}_{13}^{21}\underline{u}\right) \tag{5}$$

$$\underline{D_{in}} = \left(\mathbf{I} - \mathbf{S}_{22}\mathbf{L}\right)^{-1}\left(\mathbf{S}_{21}^{11}\underline{z} + \mathbf{S}_{21}^{12}\mathbf{X}_{GY}\underline{I_{GY}} + \mathbf{S}_{23}\underline{u}\right) \tag{6}$$

The solution of (5) and (6) are

$$\underline{I_{GY}} = \left(\mathbf{I}-\mathbf{S}_{11}^{22}\mathbf{X}_{GY}-\mathbf{S}_{12}^{21}\mathbf{M}_L\mathbf{S}_{21}^{12}\mathbf{X}_{GY}\right)^{-1}\left[\left(\mathbf{S}_{11}^{21}+\mathbf{S}_{12}^{21}\mathbf{M}_L\mathbf{S}_{21}^{11}\right)\underline{z}+\left(\mathbf{S}_{13}^{21}+\mathbf{S}_{12}^{21}\mathbf{M}_L\mathbf{S}_{23}\right)\underline{u}\right] \quad (7)$$

$$\underline{D_{in}} = \left(\mathbf{I}-\mathbf{S}_{22}\mathbf{L}-\mathbf{S}_{21}^{12}M_XS_{12}^{21}L\right)^{-1}\left[\left(\mathbf{S}_{21}^{11}+\mathbf{S}_{21}^{12}\mathbf{M}_X\mathbf{S}_{11}^{21}\right)\underline{z}+\left(\mathbf{S}_{23}+\mathbf{S}_{21}^{12}\mathbf{M}_L\mathbf{S}_{13}^{21}\right)\underline{u}\right] \quad (8)$$

where

$$\mathbf{M}_L = \mathbf{L}\left(\mathbf{I}-\mathbf{S}_{22}\mathbf{L}\right)^{-1} \quad (9)$$

$$\mathbf{M}_X = \mathbf{X}_{GY}\left(\mathbf{I}-\mathbf{S}_{11}^{22}\mathbf{X}_{GY}\right)^{-1} \quad (10)$$

By substituting (7) and (8) into the first line (1) with (3) and (4)

$$\dot{\underline{x}} = \mathbf{S}_{11}\underline{z}+\mathbf{S}_{13}^{11}\underline{u}+\mathbf{S}_{11}^{12}\mathbf{Q}_X\left[\left(\mathbf{S}_{11}^{21}+\mathbf{S}_{12}^{21}\mathbf{M}_L\mathbf{S}_{21}^{11}\right)\underline{z}+\left(\mathbf{S}_{13}^{21}+\mathbf{S}_{12}^{21}\mathbf{M}_L\mathbf{S}_{23}\right)\underline{u}\right]+\mathbf{S}_{12}^{11}\mathbf{Q}_L\left[\left(\mathbf{S}_{21}^{11}+\mathbf{S}_{21}^{12}\mathbf{M}_X\mathbf{S}_{11}^{21}\right)\underline{z}+\left(\mathbf{S}_{23}+\mathbf{S}_{21}^{12}\mathbf{M}_X\mathbf{S}_{13}^{21}\right)\underline{u}\right] \quad (11)$$

where

$$\mathbf{Q}_X = \mathbf{X}_{GY}\left[\mathbf{I}-\left(\mathbf{S}_{11}^{22}+\mathbf{S}_{12}^{21}\mathbf{M}_L\mathbf{S}_{21}^{12}\right)\mathbf{X}_{GY}\right]^{-1} \quad (12)$$

$$\mathbf{Q}_L = \mathbf{L}\left[\mathbf{I}-\left(\mathbf{S}_{22}+\mathbf{S}_{21}^{12}\mathbf{M}_X\mathbf{S}_{12}^{21}\right)\mathbf{L}\right]^{-1} \quad (13)$$

from (11) and (2), an equation state of a system modelled by multibond graphs is defined by

$$\dot{\underline{x}} = \mathbf{A}\underline{x}+\mathbf{B}\underline{u} \quad (14)$$

where

$$\mathbf{A} = \left[\mathbf{S}_{11}^{11}+\mathbf{S}_{11}^{12}\mathbf{Q}_X\left(\mathbf{S}_{11}^{21}+\mathbf{S}_{12}^{21}\mathbf{M}_L\mathbf{S}_{21}^{11}\right)+\mathbf{S}_{12}^{11}\mathbf{Q}_L\left(\mathbf{S}_{21}^{11}+\mathbf{S}_{21}^{12}\mathbf{M}_X\mathbf{S}_{11}^{21}\right)\right]\mathbf{F} \quad (15)$$

$$\mathbf{B} = \mathbf{S}_{13}^{11}+\mathbf{S}_{11}^{12}\mathbf{Q}_X\left(\mathbf{S}_{13}^{21}+\mathbf{S}_{12}^{21}\mathbf{M}_L\mathbf{S}_{23}\right)+\mathbf{S}_{12}^{11}\mathbf{Q}_L\left(\mathbf{S}_{23}+\mathbf{S}_{21}^{12}\mathbf{M}_X\mathbf{S}_{13}^{21}\right) \quad (16)$$

In the next section, the steady state response for systems modelled by multibond graphs is presented.

4 Steady State Response

When the dynamic period of a stable system has finished, the steady state response can be obtained. In order to obtain the steady state of a system, a derivative causality for the storage elements of a multibond graph is assigned (MBGD) which is shown in Fig. 8.

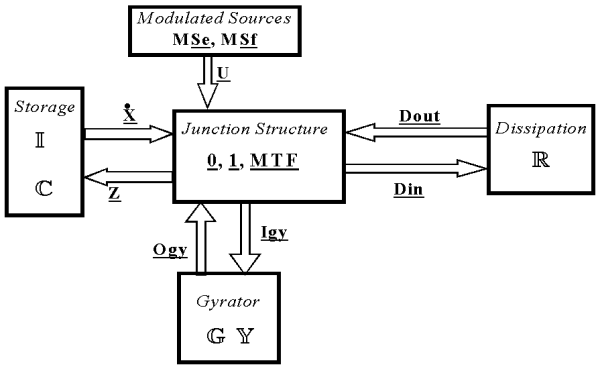

Fig. 8: Multibond graph in derivative causality assignment.

The main result of this paper is introduced in the following lemma.

Lemma 2.

Consider a multibond graph in a derivative causality assignment whose scheme is shown in Fig. 8, *where the junction structure is given by*

$$\begin{bmatrix} \underline{z} \\ \underline{I_{GY}^d} \\ \underline{D_{in}^d} \end{bmatrix} = \begin{bmatrix} \mathbf{J}_{11}^{11} & \mathbf{J}_{11}^{12} & \mathbf{J}_{12}^{11} & \mathbf{J}_{13}^{11} \\ \mathbf{J}_{11}^{21} & \mathbf{J}_{11}^{22} & \mathbf{J}_{12}^{21} & \mathbf{J}_{13}^{21} \\ \mathbf{J}_{21}^{11} & \mathbf{J}_{21}^{12} & \mathbf{J}_{22} & \mathbf{J}_{23} \end{bmatrix} \begin{bmatrix} \dot{\underline{x}} \\ \underline{O_{GY}^d} \\ \underline{D_{out}^d} \\ \underline{u} \end{bmatrix} \quad (17)$$

with

$$\underline{D_{out}^d} = \mathbf{L}^d\underline{D_{in}^d} \quad (18)$$

$$\underline{O_{GY}^d} = \mathbf{X}_{GY}^d\underline{I_{GY}^d} \quad (19)$$

the steady state response for the state variables is defined by

$$\underline{x_{ss}} = \mathbf{B}^*\underline{u_{ss}} \quad (20)$$

where

$$\mathbf{B}^* = \mathbf{F}^{-1}\left(\mathbf{J}_{13}^{11}+\mathbf{J}_{11}^{12}\mathbf{P}_x\mathbf{J}_{XB}+\mathbf{J}_{12}^{11}\mathbf{P}_L\mathbf{J}_{LB}\right) \quad (21)$$

being

$$\mathbf{J}_{XB} = \mathbf{J}_{13}^{21}+\mathbf{J}_{12}^{21}\mathbf{N}_L\mathbf{J}_{23} \quad (22)$$

$$\mathbf{J}_{LB} = \mathbf{J}_{23}+\mathbf{J}_{21}^{12}\mathbf{N}_X\mathbf{J}_{13}^{21} \quad (23)$$

and

$$\mathbf{N}_L = \mathbf{L}^d\left(\mathbf{I}-\mathbf{J}_{22}\mathbf{L}^d\right)^{-1} \quad (24)$$

$$\mathbf{N}_X = \mathbf{X}_{GY}^d\left(\mathbf{I}-\mathbf{J}_{11}^{22}\mathbf{X}_{GY}^d\right)^{-1} \quad (25)$$

$$\mathbf{P}_L = \mathbf{L}^d\left(\mathbf{I}-\mathbf{J}_{22}\mathbf{L}^d-\mathbf{J}_{21}^{12}\mathbf{N}_X\mathbf{J}_{12}^{21}\mathbf{L}^d\right)^{-1} \quad (26)$$

$$\mathbf{P}_X = \mathbf{X}_{GY}^d\left(\mathbf{I}-\mathbf{J}_{11}^{22}\mathbf{X}_{GY}^d-\mathbf{J}_{12}^{21}\mathbf{N}_L\mathbf{J}_{21}^{12}\mathbf{X}_{GY}^d\right)^{-1} \quad (27)$$

Proof. From the third line of (17) with (18) and (19)

$$\underline{D_{in}^d} = \left(\mathbf{I}-\mathbf{J}_{22}\mathbf{L}^d\right)^{-1}\left(\mathbf{J}_{21}^{11}\dot{\underline{x}}+J_{21}^{12}\mathbf{X}_{GY}^d\underline{\mathbf{I}_{GY}^d}+\mathbf{J}_{23}\underline{u}\right) \quad (28)$$

form the second line of (17) with (18) and (19)

$$\underline{I^d_{GY}} = \left(\mathbf{I} - \mathbf{J}^{22}_{11}\mathbf{X}^d_{GY}\right)^{-1}\left(\mathbf{J}^{21}_{11}\overset{\bullet}{\underline{x}} + \mathbf{J}^{21}_{12}\mathbf{L}^d\underline{D^d_{in}} + \mathbf{J}^{21}_{13}\underline{u}\right) \tag{29}$$

by solving (28) and (29)

$$\begin{aligned}\underline{D^d_{in}} &= \left(\mathbf{I} - \mathbf{J}_{22}\mathbf{L}^d - \mathbf{J}^{12}_{21}\mathbf{N}_X\mathbf{J}^{21}_{12}\mathbf{L}^d\right)^{-1}\left[\left(\mathbf{J}^{11}_{21} + \right.\right.\\ &\left.\left.\mathbf{J}^{12}_{21}\mathbf{N}_X\mathbf{J}^{21}_{11}\right)\overset{\bullet}{\underline{x}} + \left(\mathbf{J}_{23} + \mathbf{J}^{12}_{21}\mathbf{N}_X\mathbf{J}^{21}_{13}\right)\underline{u}\right] \end{aligned}\tag{30}$$

$$\begin{aligned}\underline{I^d_{GY}} &= \left(\mathbf{I} - \mathbf{J}^{22}_{11}\mathbf{X}^d_{GY} - \mathbf{J}^{21}_{12}\mathbf{N}_L\mathbf{J}^{12}_{21}\mathbf{X}^d_{GY}\right)^{-1}\left[\left(\mathbf{J}^{21}_{11} + \right.\right.\\ &\left.\left.\mathbf{J}^{21}_{12}\mathbf{N}_L\mathbf{J}^{11}_{21}\right)\overset{\bullet}{\underline{x}} + \left(\mathbf{J}^{21}_{13} + \mathbf{J}^{21}_{12}\mathbf{N}_L\mathbf{J}_{23}\right)\underline{u}\right] \end{aligned}\tag{31}$$

from the first line of (17) with (30) and (31)

$$\begin{aligned}\underline{z} &= \mathbf{J}^{12}_{11}\mathbf{X}^d_{GY}\left(\mathbf{I} - \mathbf{J}^{22}_{11}\mathbf{X}^d_{GY} - \mathbf{J}^{21}_{12}\mathbf{N}_L\mathbf{J}^{12}_{21}\mathbf{X}^d_{GY}\right)^{-1}\left[\left(\mathbf{J}^{21}_{11}\right.\right.\\ &\left.\left.+\mathbf{J}^{21}_{12}\mathbf{N}_L\mathbf{J}^{11}_{21}\right)\overset{\bullet}{\underline{x}} + \left(\mathbf{J}^{21}_{13} + \mathbf{J}^{21}_{12}\mathbf{N}_L\mathbf{J}_{23}\right)\underline{u}\right] + \mathbf{J}^{11}_{11}\overset{\bullet}{\underline{x}}\\ &+J^{11}_{12}L^d\left(\mathbf{I} - \mathbf{J}_{22}\mathbf{L}^d - \mathbf{J}^{12}_{21}\mathbf{N}_X\mathbf{J}^{21}_{12}\mathbf{L}^d\right)^{-1}\left[\left(\mathbf{J}^{11}_{21} + \right.\right.\\ &\left.\left.\mathbf{J}^{12}_{21}\mathbf{N}_X\mathbf{J}^{21}_{11}\right)\overset{\bullet}{\underline{x}} + \left(\mathbf{J}_{23} + \mathbf{J}^{12}_{21}\mathbf{N}_X\mathbf{J}^{21}_{13}\right)\underline{u}\right] + J^{11}_{13}\underline{u}\end{aligned}\tag{32}$$

from (26), (27) and (32)

$$\begin{aligned}\underline{z} &= \left[\mathbf{J}^{11}_{11} + \mathbf{J}^{12}_{11}\mathbf{P}_X\left(\mathbf{J}^{21}_{11} + \mathbf{J}^{21}_{12}\mathbf{N}_L\mathbf{J}^{11}_{21}\right) + \right.\\ &\left.\mathbf{J}^{11}_{12}\mathbf{P}_L\left(\mathbf{J}^{11}_{21} + \mathbf{J}^{12}_{21}\mathbf{N}_X\mathbf{J}^{21}_{11}\right)\right]\overset{\bullet}{\underline{x}} + \left[J^{11}_{13}\right.\\ &\left.+\mathbf{J}^{12}_{11}\mathbf{P}_X\left(\mathbf{J}^{21}_{13} + \mathbf{J}^{21}_{12}\mathbf{N}_L\mathbf{J}_{23}\right) + \mathbf{J}^{11}_{12}\mathbf{P}_L\right.\\ &\left.\left(\mathbf{J}_{23} + \mathbf{J}^{12}_{21}\mathbf{N}_X\mathbf{J}^{21}_{13}\right)\right]\underline{u}\end{aligned}\tag{33}$$

then (33) can be written by

$$\underline{x} = \mathbf{A}^*\overset{\bullet}{\underline{x}} + \mathbf{B}^*\underline{u} \tag{34}$$

where

$$\begin{aligned}\mathbf{FA}^* &= \mathbf{J}^{11}_{11} + \mathbf{J}^{12}_{11}\mathbf{P}_X\mathbf{J}_{XA} + \mathbf{J}^{11}_{12}\mathbf{P}_L\mathbf{J}_{LA}\\ \mathbf{FB}^* &= \mathbf{J}^{11}_{13} + \mathbf{J}^{12}_{11}\mathbf{P}_X\mathbf{J}_{XB} + \mathbf{J}^{11}_{12}\mathbf{P}_L\mathbf{J}_{LB}\end{aligned}$$

being $\mathbf{J}_{XA} = \mathbf{J}^{21}_{11} + \mathbf{J}^{21}_{12}\mathbf{N}_L\mathbf{J}^{11}_{21}$ and $\mathbf{J}_{LA} = \mathbf{J}^{11}_{21} + \mathbf{J}^{12}_{21}\mathbf{N}_X\mathbf{J}^{21}_{11}$ with $\mathbf{J}_{XB}$ and $\mathbf{J}_{LB}$ defined by (22) and (23), respectively. Now, (34) is re-written by

$$\overset{\bullet}{\underline{x}} = \left(\mathbf{A}^*\right)^{-1}\underline{x} - \left(\mathbf{A}^*\right)^{-1}\mathbf{B}^*\underline{u} \tag{35}$$

by comparing (14) with (35), the relationships between MBGI and MBGD are

$$\mathbf{A}^* = \mathbf{A}^{-1} \tag{36}$$

$$\mathbf{B}^* = -\mathbf{A}^{-1}\mathbf{B} \tag{37}$$

for the steady state response $\overset{\bullet}{\underline{x}} = 0$ and using (14)

$$\underline{x_{ss}} = -\mathbf{A}^{-1}\mathbf{B}u \tag{38}$$

and from (37) and (38), equation (20) is proved. ■

In the next section, the proposed methodology is applied to an example.

5 Example

A three-phase electrical system formed by two sources and a transmission line for each phase is shown in Fig. 9.

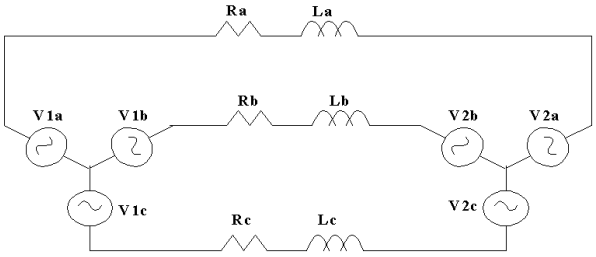

Fig. 9: Three-phase electrical system.

The corresponding multibond graph of the electrical system is shown in Fig. 10.

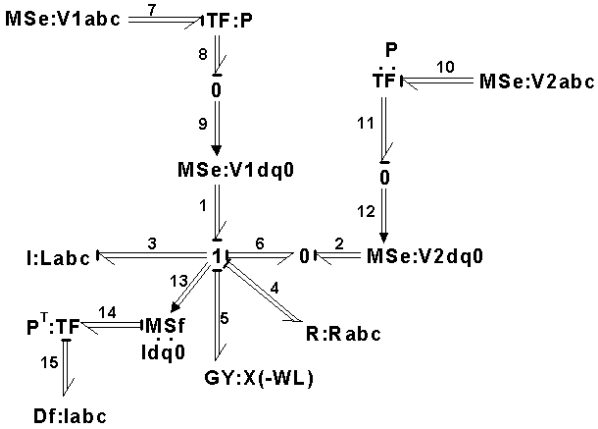

Fig. 10: MBGI of the electrical system.

The key vectors of the multibond graph are

$$\begin{aligned}\underline{x} &= \underline{p_3};\ \overset{\bullet}{\underline{x}} = \underline{e_3};\ \underline{z} = \underline{f_3};\ \underline{D_{in}} = \underline{f_4};\ \underline{D_{out}} = \underline{e_4}\\ \underline{I_{GY}} &= \underline{f_5};\ \underline{O_{GY}} = \underline{e_5};\ \underline{u} = \left[\begin{array}{cc}\underline{e_1} & \underline{e_2}\end{array}\right]^T\end{aligned}$$

and the constitutive relations are

$$\mathbf{F} = diag\left\{R_e,\ R_e,\ R_e\right\} = \mathbf{R}_e \tag{39}$$

$$\mathbf{L} = diag\left\{L_e,\ L_e,\ L_e\right\} = \mathbf{L}_e \tag{40}$$

$$\mathbf{X}_{GY} = \mathbf{X}\left(-wL\right) = \left[\begin{array}{ccc}0 & wL_a & 0\\ wL_b & 0 & 0\\ 0 & 0 & 0\end{array}\right] \tag{41}$$

The junction structure of this multibond graph in an integral causality assignment is

$$\left[\begin{array}{c}\underline{e_3}\\ \underline{f_5}\\ \underline{f_4}\end{array}\right] = \left[\begin{array}{ccccc}0 & -\mathbf{I} & -\mathbf{I} & \mathbf{I} & -\mathbf{I}\\ \mathbf{I} & 0 & 0 & 0 & 0\\ \mathbf{I} & 0 & 0 & 0 & 0\end{array}\right]\left[\begin{array}{c}\underline{f_3}\\ \underline{e_5}\\ \underline{e_4}\\ \underline{e_1}\\ \underline{e_2}\end{array}\right] \tag{42}$$

From (14), (15), (16) with (39) to (42), the state equation of the electrical systems is

$$\dot{\underline{x}} = -\left[\mathbf{R}_e + \mathbf{X}\left(-wL\right)\right]\mathbf{L}_e^{-1} + \underline{e_1} - \underline{e_2} \qquad (43)$$

The corresponding MBGD of the system is shown in Fig. 11.

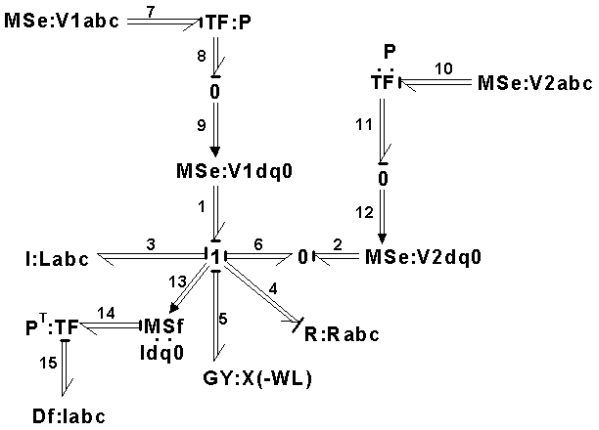

Fig. 11: MBGD of the electrical system.

The key vectors for the dissipation elements are

$$\underline{D_{in}^d} = \underline{e_4};\ \underline{D_{out}^d} = \underline{f_4}$$

and the constitutive relation is

$$\mathbf{L}^d{=}diag\left\{L_e^{-1},\ L_e^{-1}, L_e^{-1}\right\} = \mathbf{L}_e^{-1} \qquad (44)$$

The junction structure of the MBGD is

$$\begin{bmatrix} \underline{f_3} \\ \underline{f_5} \\ \underline{e_4} \end{bmatrix} = \begin{bmatrix} 0 & \mathbf{0} & \mathbf{I} & \mathbf{0} & 0 \\ \mathbf{0} & 0 & \mathbf{I} & 0 & 0 \\ -\mathbf{I} & -\mathbf{I} & 0 & \mathbf{I} & \mathbf{I} \end{bmatrix} \begin{bmatrix} \underline{e_3} \\ \underline{e_5} \\ \underline{f_4} \\ \underline{e_1} \\ \underline{e_2} \end{bmatrix} \qquad (45)$$

From (20), (21) with (39), (39), (44) and (45)

$$\begin{aligned} \underline{x_{ss}} &= \begin{bmatrix} \frac{L_e R_e}{R_e^2+w^2L_e^2} & \frac{-wL_e^2}{R_e^2+w^2L_e^2} & 0 \\ \frac{-wL_e^2}{R_e^2+w^2L_e^2} & \frac{L_e R_e}{R_e^2+w^2L_e^2} & 0 \\ 0 & 0 & \frac{L_e}{R_e} \end{bmatrix} \begin{bmatrix} v_1^d - v_2^d \\ v_1^q - v_2^q \\ v_1^0 - v_2^0 \end{bmatrix} \\ &= \begin{bmatrix} \left(p_3^d\right)_{ss} \\ \left(p_3^q\right)_{ss} \\ \left(p_3^0\right)_{ss} \end{bmatrix} \end{aligned} \qquad (46)$$

The numerical parameters of this system are: $R_e = 5\Omega$, $L_e = 0.1H$, $F = 60Hz$, $v_1^{abc} = \begin{bmatrix} 200\cos\left(377t\right) \\ 200\cos\left(377t-120\right) \\ 200\cos\left(377t+120\right) \end{bmatrix} V$ and $v_2^{abc} = \begin{bmatrix} 100\cos\left(377t\right) \\ 100\cos\left(377t-120\right) \\ 100\cos\left(377t+120\right) \end{bmatrix}$

The simulation results by using 20-SIM software of the MBGI are shown in Figs. 12 and 13.

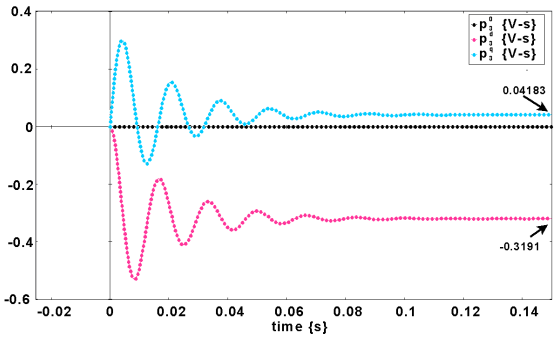

Fig. 12: Response for $\underline{p_3}$.

By substituting the numerical values into (46)

$$\underline{x_{ss}} = \begin{bmatrix} \left(p_3^d\right)_{ss} \\ \left(p_3^q\right)_{ss} \\ \left(p_3^0\right)_{ss} \end{bmatrix} = \begin{bmatrix} -0.3191 \\ 0.04233 \\ 0 \end{bmatrix} V - s \qquad (47)$$

It can be shown that the response obtained by (47) is successful respect to the simulation results of Fig. 12.

The (a, b, c) components for the electrical current by applying the Park´s transformation is shown in Fig. 13.

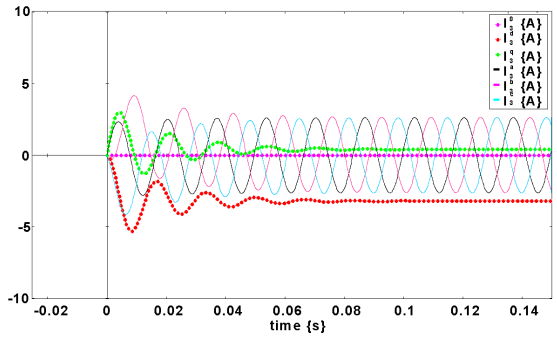

Fig. 13: Response for the $(a, b.c)$ electrical current.

Finally, the analysis and methodologies developed for bond graphs using the junction structure can be extended with this paper for multibond graphs.

6 Conclusions

A junction structure of multibond graphs has been proposed. Hence, the mathematical model of multibody systems modelled by multibond graphs can be obtained. In order to obtain the steady state response, a multibond graph in a derivative causality assignment is proposed. An example using the proposed methodology have been solved. The advantages for applying multibond graphs respect bond graphs for multibody systems are clear: short notation, compact junction structure and mathematical model. Also, the proposed

junction structure to determine characteristics (nonlinear observability, controllability, stability, control design) in the physical domain can be the key for new results.

References

[1] X-S Ge, W-J Zhao, L-Q Chen and Y.-Z Liu, Symbolic Linearization of Differential/Albegraic Equations Based on Cartesian Coordinates,, *Techische Mechanik,* Band 25, Heft 3-4, (2005), 230-240.

[2] M. J. L. Tiernego and A. M. Bos, Modelling the Dynamics and Kinematics of Mechanical Systems with Multibond Graphs, Journal of the Franklin Institute, Vol. 319, No. 1/2, pp. 37-50, January/Febraury, 1985.

[3] R. R. Allen, Multiport Representation of Inertia Properties of Kinematic Mechanisms, *J. of the Franklin Inst.*, Vol. 308, No.3 pp. 235-253, 1979.

[4] M. J. L. Tiernego and J. J. Van Dixhoorn, Three-Axis Platform Simulation: Bond Graph and Lagrangian Approach, *J. of the Franklin Inst.,* Vol. 308, No.3, pp. 185-204, 1979.

[5] P. C. Breedveld, Multibond Graph Elements in Physical Systems Theory, *J. of the Franklin Inst.,* Vol. 319, No. 1/2, pp. 1-36, 1985.

[6] P. C. Breedveld, Stability of rigid body rotation from a bond graph perspective, *Simulation Practice and Theory,* 17 (2009) 92-106.

[7] P. C. Breedveld, Decomposition of Multiport Elements in a Revised Multibond Graph Notation, *J. of the Franklin Inst.,* Vol. 318, No. 4, pp.253-273, 1984.

[8] Dean C. Karnopp, Donald L. Margolis and Ronald C. Rosenberg, *System Dynamics Modeling and Simulation of Mechatronic Systems*, Wiley, John & Sons, 2000.

[9] C. Sueur and G. Dauphin-Tanguy, "Bond graph approach for structural analysis of MIMO linear systems", *Journal of the Franklin Institute*, Vol. 328, No. 1, pp. 55-70, 1991.

[10] P. Breeveld, A bond graph algorithm to determine the equilibrium state of a system, *Journal of the Franklin Institute,* 1984, 318, 71-75.

[11] E. Bideaux, W. Marquis-Favre and S. Scavarda, Equilibrium set investigation using bicausality, *Math. Comput. Model Dynam. Syst.,* 12(2), 127-140.

[12] G. Gonzalez and R. Galindo, Steady state determination using bond graphs for systems with singular state matrix, *Proc. InstMech Engineers, Part I: Journal of Systems and Control Engineering,* 2011, 225:885.